Formulation and characterization of Curcumin-Loaded Silver Nanoparticle Hydrogel Patches in Modulating Cellular Responses during Wound Healing

Nisha Thakre¹, Gaurav Tiwari², Naveen Gupta³, Dharmendra Rajput⁴ 1.2,3,4 Madhyanchal professional university, Bhopal, M. P

^{2,3,4}Madhyanchal professional university, Bhopal, M. P Corresponding email: nishathakre81@gmail.com

Abstract:

Objective: The study aimed to develop a hydrogel containing silver nanoparticles (AgNPs) loaded with curcumin to evaluate its antimicrobial and wound healing activity. The primary goal was to optimize the formulation and assess its efficacy in promoting wound healing in an animal model.

Methodology: Silver nanoparticles were synthesized using silver nitrate, tri-sodium citrate as a stabilizer, and sodium borohydride as a reducing agent. The nanoparticles were isolated, purified, and characterized for size and charge using zeta sizer, yielding an average particle size of 54 nm with a polydispersity index of 0.2 and zeta potential of -16 mV. Optimization was conducted by varying concentrations of AgNO3, TSC, NaBH4, and stirring time, with the best formulation achieving 75.2% entrapment efficiency. The optimized nanoparticles were loaded into a carbopol hydrogel and subjected to Fourier Transform Infrared Spectroscopy (FTIR) to confirm curcumin entrapment. The hydrogel's release profile was studied, and in-vivo wound healing activity was evaluated using an excision model in animals.

Results: The optimized hydrogel exhibited a pH range of 5.3–7.8 and good spreadability. In-vivo studies showed significant wound contraction, with 98-100% contraction in AgNP-treated groups by day 15. The tensile strength of wounds treated with the hydrogel was higher than in control groups, indicating effective healing. The hydrogel followed the Korsmeyer-Peppas model for curcumin release. The study suggests further research could improve drug release and explore additional natural ingredients for enhanced wound healing.

Keywords: Silver nanoparticles, Curcumin, Hydrogel formulation, Wound healing, Nanoparticle

1. Introduction

1.1 Background

Wound healing disorders, characterized by prolonged inflammation, impaired re-epithelialization, and delayed tissue remodelling, can lead to severe complications including infections, amputations, and even death in extreme cases. Chronic wounds affect millions of people globally, with an estimated 6.5 million patients in the U.S. alone, costing the healthcare system billions of dollars annually. The rising prevalence of diabetes and an aging population further exacerbates the issue, highlighting the urgent need for novel wound care therapies that can promote faster and more efficient healing.(1)

1.2 Challenges in Wound Healing

Factors including poor vascularization, prolonged inflammation, microbial infection, and impaired cellular responses such as fibroblast proliferation, collagen deposition, and keratinocyte migration causes delay in wound healing. Chronic wounds are also often associated with biofilm formation by pathogenic bacteria, which can further impede healing by creating a barrier that limits the penetration of conventional antibiotics (Wu et al., 2017). Traditional treatments, such as moist dressings, antibiotics, and growth factors, have limited efficacy in addressing these complex challenges. Furthermore, the overuse of antibiotics has led to an increase in antimicrobial resistance (AMR), making it difficult to control infections in chronic wounds. (2)

1.3 Curcumin: A Natural Bioactive Compound with Potent Wound Healing Properties

Curcumin has been extensively studied for its ability to modulate various molecular pathways involved in wound healing, including the nuclear factor kappa-light-chain-enhancer of activated B cells (NF- κ B), mitogen-activated protein kinase (MAPK), and transforming growth factor-beta (TGF- β) signaling pathways. These pathways play crucial roles in regulating inflammation, fibroblast proliferation, and collagen synthesis, which are essential for tissue repair.(3)

Several studies have demonstrated that curcumin can enhance wound healing by accelerating the granulation tissue formation, promoting collagen deposition, and improving re-epithelialization. However, despite its therapeutic potential, the clinical application of curcumin is limited by its poor water solubility, rapid degradation, and low bioavailability. These challenges necessitate the development of innovative delivery systems that can improve the stability, bioavailability, and therapeutic efficacy of curcumin in wound healing applications.(4)

1.4 Silver Nanoparticles (AgNPs) as a Potent Antimicrobial Agent for Wound Healing

Silver nanoparticles (AgNPs) are well-known for their potent antimicrobial activity, making them an attractive option for use in wound dressings to prevent infections. AgNPs exert their antimicrobial effects through multiple mechanisms, including the disruption of bacterial cell membranes, generation of reactive oxygen species (ROS), and interaction with bacterial DNA, ultimately leading to cell death. (5)

In addition to their antimicrobial properties, AgNPs have been shown to promote wound healing by enhancing fibroblast migration, collagen synthesis, and angiogenesis. However, like curcumin, AgNPs also face challenges related to stability and potential toxicity, particularly at high concentrations. Therefore, the incorporation of AgNPs into biocompatible delivery systems, such as hydrogels, has emerged as a promising strategy to maximize their therapeutic benefits while minimizing potential adverse effects.(6)

Recent studies have shown that hydrogel patches containing nanoparticles can significantly enhance wound healing by providing a sustained release of bioactive agents, maintaining optimal moisture levels, and protecting the wound from microbial infections. For instance, Study demonstrated that a hydrogel containing AgNPs accelerated wound closure and improved tissue regeneration in a diabetic rat model.(7) Similarly, hydrogel systems incorporating curcumin have been shown to enhance collagen deposition, reduce oxidative stress, and promote re-epithelialization. This study focuses on formulation and evaluation of hydrogel patch incorporating silver nanoparticle loaded with curcumin.

2. Material and Method

2.1 Materials

Silver nitrate was obtained from Loba Chemie, Mumbai, Tri-sodium citrate and Curcumin (pure) was obtained from HiMedia, Mumbai. Carbopol 940 and Methanol was procured from Rankem India Ltd. Ingredients used in culture media like Nutrient agar and Agar agar was obtained from Loba Chemie, Mumbai. Type 1 (Milli Q) distilled water was used in the study.

2.2 Methods

2.2.1 Preparation of Silver Nanoparticles(9)

Silver nanoparticles were formulated through silver nitrate solution by chemical reduction method. 5 mL of tri-sodium citrate (TSC) 0.05 M and 5 mL of silver nitrate1 mM were added to 185 mL of water type 1 and stirred for 3 minat 3000 RPM. 5 mL of sodium borohydride0.05 Mand 75 mL curcumin solution (0.25 mg/ ml,4:6 acetone:distilled water) wasdripped slowly. pH was adjusted to 10 using sodium hydroxide solution and reaction mixture was allowed to stir until colour change occur from yellow to dark brownindicating the formation of AgNPs. Prepared silver nanoparticles were obtained through centrifugation at 5000rpm. (10) Optimized parameter were taken for the formulation of silver nanoparticles as per our previous research. (11)

2.2.2 Preparation of Silver nanoparticle incorporated hydrogel patch

Silver nanoparticle incorporated hydrogel patch were prepared using carbopol as a polymer. Varying concentration of carbopol and different grades of carbopol were used for the preparation and optimization of hydrogel patch. Hydrogel patch were prepared by the following procedure: carbopol resin was dispersed in purified water in which propylene glycol (15%,w/w), edetate disodium (0.15%, w/w), and the preservatives were previously added and left to stay for 24 h.(12) The mixture was

stirred the next day (500 rpm/min, 15 min) until the carbopol resin was homogeneously dispersed and then neutralized by addition of an accurate amount of 18%, w/w, solution of sodium-hydroxide (solution of sodium-hydroxide: carbopol = 2.3:1, w/w). In order to obtain silver nanoparticles loaded hydrogel previously prepared silver nanoparticles were incorporated into previously prepared carbopol hydrogel patches in the ratio 2:1, w/w, by mixing them into the gel by an electrical mixer at 200 rpm/min for 5 min.(13)

Table 1: Optimization of hydrogel patch formulation

Sl. No	Formulation	Carbopol Conc	Propylene Glycol	Sodium Edetate
1	HF1	0.5%	15%	0.15%
2	HF2	1%	15%	0.15%,
3	HF3	1.5%	15%	0.15%,
4	HF4	2%	15%	0.15%,
5	HF5	1%	15%	0.05%
6	HF6	1%	15%	0.10%
7	HF7	1%	15%	0.15%
8	HF8	1%	15%	0.20%

3. Evaluation of Silver nanoparticles containing Curcumin

3.1 Dynamic Light Scattering (DLS) analysis

The size of the obtained silver nanoparticle was determined using a Zetasizer Nano ZSP (ZEN 5600) study using dynamic light scattering (DLS). This method involves the passage of a monochromatic light (laser) through a solution of nanoparticles moving in Brownian motion. When the light strikes a moving particle, it produces a Doppler shift, which modifies the wavelength of the incoming light. The size of the particle has an impact on this alteration.(14)

3.2 Zeta potential of biosynthesized AgNPs

Both the type and strength of a nanoparticle's surface charge influence how it interacts with the biological environment and how it interacts electrostatically with bioactive substances. The potential difference between the outer Helmholtz plane and the shear surface is represented by the zeta potential, an indirect measure of surface charge. To guarantee stability and prevent particle aggregation, high zeta potential values—either positive or negative—should be attained.(15)The zeta potential of the nanoparticles was determined with a ZetasizerNanoZS instrument from Malvern Co. Ltd., the UK equipped with a He-Ne laser.Zeta potential values are determined from the electrophoretic mobility of the particleswith the laser Doppler technique. The samples were dispersed in Milli Q water. (16)

3.3 UV-VIS Spectra Analysis

UV-Vis sprectrum were used for reduction media sample at different time intervals for identification of reduction of pure Ag⁺ions, the samples were compared to 1 mL of distilled water used as blank.Shimadzu 1700 UV/Vis spectrophotometerwas used to perform UV-Vis spectral analysis at a resolution of 1 nm from 200 to 800 nm. The absorption peaks at 420–450 nm areas were seen and recorded, and they are identical to the features of the metallic silver UV-visible spectrum.(17)

3.4 FT-IR Measurements

Fourier transformed infrared radiation spectroscopy studies were performed to determine the potential biomolecules responsible for the reduction of the Ag⁺ ions and formation of AgNPs. To exclude the unentrapped curcumin and unreacted silver nitrate, AgNPs were redispersed three times with sterile deionized water. After re-dispersion, AgNPs solution was centrifuged for 30 minutes at 3000 rpm and finally the obtained sediment was lyophilized to obtain AgNPs powder. The samples were ground using KBr pellets after being baked in an oven for a whole night at 60°C. They were then examined using a Bruker Tensor 27 model in the diffuse reflectance mode, which operated at a resolution of 4 cm⁻¹.(18)

3.5 Evaluation of curcumin-AgNPs hydrogel

3.5.1 Color, appearance & homogeneity

Visual inspection checked the formulations for their color, appearance, and homogeneity. (19)

3.5.2 pH& viscosity

A digital pH meter (PR-11, Sartorius) was used to evaluate the gels for their pH. 1 g of the gel was combined with 100 ml of water to measure pH, and the mixture was then kept at 4° C for two hours. All measures were done three times, and the average values were recorded. Using spindle No. 63 at 200 rpm and a Brookfield Viscometer (DV II RVTDV-II), the viscosity of the gel compositions was measured. Before taking measurements, the gel samples were allowed to settle for 30 minutes at $25\pm1^{\circ}$ C.(20)

3.5.3 Spreadability

For spreadability determination of gel formulations, the spreading diameter of 1 g of gel sandwiched between two horizontal plates after one minute was measured. The upper plate's typical weight was 125 g.(21)

3.5.4 Extrudability

The method used to assess gel extrudability was based on the amount of gel extruded from a tube as a percentage when a given load was applied. The understudy formulation was placed in a collapsible tube with a 5 mm tip aperture. To discharge gel through the opening in the tube, a 50 g weight was positioned at the bottom. The amount of gels extruded via the tip was weighed, computed, and reported to measure extrudability. (22)

3.5.5 Rheological properties of Carbopol hydrogel

Dynamic-Hybrid Rheometer(TA Instruments, New Castle, DE) along with cone plate fixture (40 mm cone diameter and cone angle of 1.99°) was used to perform rheological examination of Carbopol hydrogels. Temperature was controlled by peltier heating system. The TRIOS software (version 2.6.1, TA Instruments, New Castle, DE) of Dynamic-Hybrid Rheometer was used for dataanalysis. Prior to the rheological experiment, Carbopol hydrogel formulation was placed on the peltierplate just sufficient enough to cover the cone at the top of the plate. The Carbopol hydrogel on the peltier plate was then equilibrated at a controlled temperature (depending upon the experimental condition) for 3 min both before and after lowering the cone over the peltier plate. After lowering thecone, the gap between cone and plate was trimmed with "trim gap" option in the rheometer to provide thin uniform film of the Carbopol hydrogel under the cone. The excess Carbopol hydrogel on the sides of the cone was removed carefully without disturbing the film between plate and cone. Following tests were then performed for the hydrogel formulations. (23)

3.6 Characterization of hydrogel patches:

3.6.1 Swelling properties and gel content:

Properties on swelling were conducted with respect to gel content and an equilibrium swelling ratio. Studies on swelling were conducted independently for both formulations in pure water. The lyophilized hydrogels were divided into discs of 8 x 2 mm and then weighed. After that, distilled water was submerged in these hydrogel discs. Swollen discs were taken out at regular times interval, additional surface water was eliminated with the use of filter paper, weighed on an analytical scale (n = 3) and again dipped into the same distilled water. The procedure was carried out repeatedly until equilibrium was reached. The hydrogel discs were dried in an oven at 38 to 40 °C until the constant weight was obtained once equilibrium was reached. (24)

3.6.2 Equilibrium swelling ratio (% ESR):

The investigation of swelling was carried out until balance was reached. The swelling ratio is explained as "The fractional growth in the hydrogel's weight due to water captivation." (24)

The following calculation was used to compute the equilibrium swelling ratio (% ESR).

% $ESR = W_{te}-W_{ti}/W_{ti} \times 100$

Where,

 W_{te} = weight of the hydrogels after swelling in distilled water

W_{ti} = weight of lyophilized hydrogels before swelling

3.6.3 Gel content (%).

When drying was completed the hydrogel discs to a fixed weight, the gel content was determined using the following equation.(24)

% Gel content = $W_t/W_d \times 100$

Where,

 W_t = weight of dry hydrogel discs

W_d = Initial weight of hydrogel discs

3.6.4 Uniformity thickness of patch

The thickness of hydrogel patches were measured using a micrometer screw gauge in mm. Thickness measurements were taken at three locations on the patch and the mean value was computed for both hydrogel patches.(25)

3.6.5 Release of curcumin-AgNPs hydrogel Patch

In order to study the release pattern of curcumin from the loaded hydrogels, a known weight of curcumin loaded hydrogel is placed in 50 ml of 7.4 pH phosphate buffer at 37 $^{\circ}$ C temperature. The released amount of curcumin is determined at different time intervals by recording the absorbance of the release medium by using UV–Vis spectrophotometer ELICO SL 164 Model (The Elico Co, Hyderabad, India). The absorption of the solutions is measured at k_{max} 491.2 nm.(26)

3.7 Wound healing Activity

3.7.1 Animal care and handling

The experiment was carried out on Wistar albino rats of 4 months, of both sexes, weighing between 120 to 170 gm. They were provided from Animal house, Lakshmi Narayan College of Pharmacy, Bhopal, (M.P.). The animals were acclimatized to the standard laboratory conditions in cross ventilated animal house at temperature 25±2°C relative humidity 44 –56% and light and dark cycles of 12:12 hours, fed with standard pallet diet and water *ad libitum* during experiment. The experiment was approved by the Institutional Animal Ethics Committee and as per CPCSEA guidelines (approval no. LNCP/IAEC/2023/007).(27)

3.7.2 Requirements:-

Scale, Surgical blades (No.18), Ketamine (anesthetics), 5%W/W Aquacel® Ag, Annie French, (Hair remover cream), Forceps, Cotton.

3.7.3 Excision model

3.7.3.1 Experimental Design

In the experiment, a total of 24 rats were used. The rats were divided into 4groups, comprising of 6 animals in each group as follows:(28)

Group I:Left untreated and considered as control.

Group II:Served as reference standard and treated with 5%w/wAquacel® Ag daily for 15 days.

Group III: Treated with Silver nano particles (Test-1) daily for 15 days

Group IV: Treated with Silver nano particles (Test-2) daily for 15 days

3.7.3.2 Procedure

The wound was created using excision method. For this hair were removed from the posterior sides of rats using hair remover cream. An area about of 10mm diameter was measured with sterile scale and this area was marked with a marker pen. The rats were anesthetized with ketamine (100mg/kgim). After 15 minutes of anaesthesia, the marked area of skin was excised with the help of surgical blade no. 18 and forceps. The skin was removed after creating the wound 500 mm². The gel, film and Intadine were applied, starting from the day of the operation, till complete epithelialisation time. The parameters studied were wound closure and epithelialisation time. The wound was measured using transparency paper, a marker, scale and area was calculated. The period of epithelialisation was calculated as the number of days required for falling of the dead tissue remnants of the wound without any residual raw wound.(28)

The percentage wound contraction was determined using the following formula:

 $Percentage of wound contraction = \underline{Initial \ wound \ size - Specific \ day \ wound \ size} \times 100$

Initial wound size

3.7.4 Incision model

The animals were grouped and treated as mentioned in excision model. The rats were anesthetized with ketamine (100mg/kg im). Paravertebral incision of 6cm length was made through the entire thickness of the skin, on either side of the vertebral column with the help of a sharp scalpel. After

complete haemostasis, the wound was closed by means of interrupted sutures placed at approximately 1cm apart. For stitching, stitched with black silk surgical thread (no. 000) and a curved needle (no. 11) were used. Animal were treated daily, as mentioned above under excision wound model from 0th day to 9th post-wounding day. One day before performing the experiment (measurement of breaking strength) the sutures were removed from the stitched wounds of rats after recovery. The wound breaking strength was measured on 10th post wounding day.(29)

4. Result and Discussion

4.1 Preparation of Silver Nanoparticles

The formation of silver nanoparticles occurs with particle size diameter varying from several nanometer that was be identified by their special optical properties due to intense absorption at 450 nm (A450) and percentage transmittance at 660 nm (T660). (1)Formation of silver nanoparticles were confirmed by the colour change and the mixture changed fromtransparent to pale yellow indicating the formation of AgNPs. The coalescence of atoms led to formation of metalclusters, which were normally stabilized byligands, surfactants or polymers by using NaBH₄ as reducing agent. These changes showed the formation of Ag NPs.

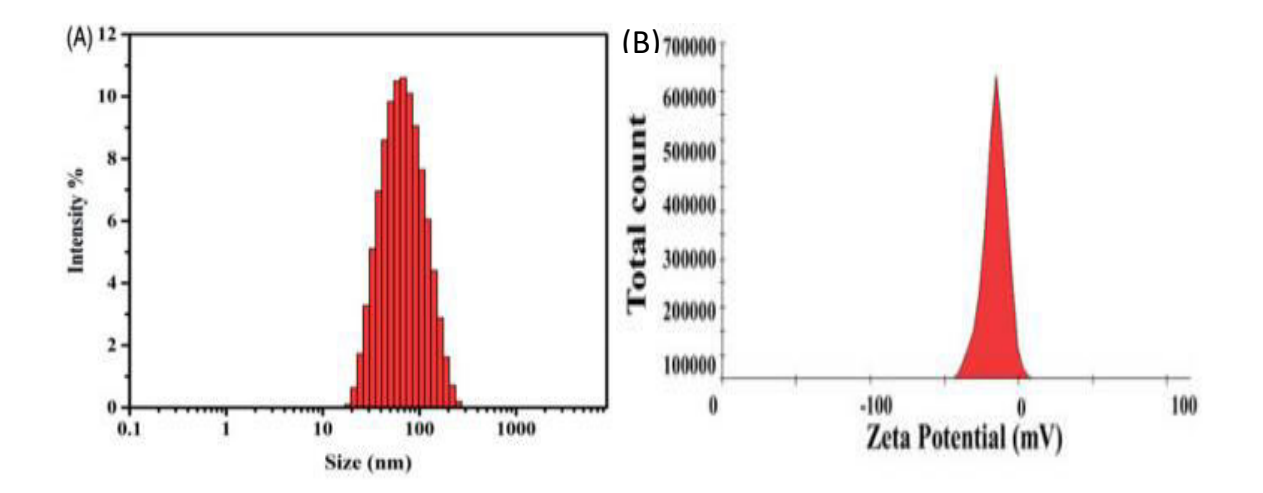
4.2 Particle Size distribution

Zetasizer analysis was performed on freshly produced AgNPs for physicochemical characterisation. The diameter of the obtained silver nanoparticles ranged from 20 to 300 nmshown in Fig 1. It was discovered that the concentration of silver in the range of 250–1000 ppm. Ag had no bearing on the size of silver nanoparticles that were produced in aqueous solutions using PVA as stabilizer. The average particle size of 54 nm and a polydispersive index of 0.2 were discovered for the optimized formulation, which amply demonstrates the homogeneity of the AgNPs that were synthesized in terms of size. These nanoparticles' determined zeta potential (-16 mV) was discovered to be within a sizable range shown in fig 2.(30)

The average size of thousands of particles per second is quantitatively measured using the data obtained from the DLS approach.SEM, on the other hand, provides qualitative information on the shape and size of a small number of particles at one particular instant.SEM data therefore showed that the manufactured nanoparticles were between 10 and 50 nm in size. The image unequivocally demonstrates that nearly all of these nanoparticles were spherical in shape and were not aggregated. The presence of AgNPs was confirmed by an absorption spectra obtained at 3 KeV, which produced a prominent peak in the silver region. A prominent peak in the EDS spectrum indicates the distinctive absorption of silver metal. The graph's lone silver element peak indicates that no contaminants may have interfered with the synthesis of AgNPs.(13)

Table 2: Evaluation of silver nanoparticles for incorporation into hydrogel patch

Particle (nm)	Size	Entrapment (%)	efficiency	Drug content (%)	Poly-dispersity index*
54.3±1.2		75.2±0.8		72.92±0.65	0.162 ± 0.029



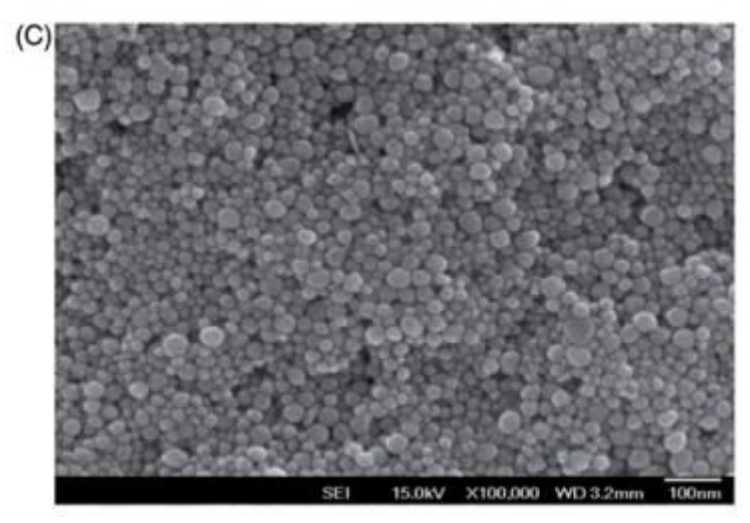


Fig 1: (A) Average particle size of optimized Silver nanoparticle observed by Dynamic light scattering. (B) Zeta potential of obtained optimized silver nanoparticle.(C) SEM data for optimized silver nanoparticles.

4.3 FTIR spectroscopy:

AgNP-containing curcumin and curcumin were both subjected to FTIR spectroscopy. The acquired data were analyzed in order to determine whether different functional groups involved in the synthesis of AgNPs and capping might interact.10 mg of the dried sample and 100 mg of KBr were used to create the transparent disk using the dried samples. The spectra were obtained by IR scanning between 450 and 4000 cm⁻¹. The extract's infrared spectrum displays a peak at 3445 cm⁻¹, indicating the presence of phenolic and alcoholic compounds as well as N–H stretching of amino groups. The following functional groups are also present: alkyl halides (658 cm⁻¹), aliphatic amines (1070.6 cm⁻¹), aromatic compounds (1422.9 cm⁻¹), and alkanes (2908 cm⁻¹). The presence of phenolic compounds (3477 cm⁻¹) in the synthesis of AgNPs is also shown by the AgNPs IR spectra; however, the upward shift of this peak suggests that phenolic compounds are the cause of the reduction into AgNPs. Additionally included are aromatic compounds (1590.9 cm⁻¹) and aldehydes (2403.9 cm⁻¹). The presence of primary and secondary amines, which are in charge of capping and stabilizing synthesized AgNPs, is shown by the peak at 832 cm⁻¹.(19)

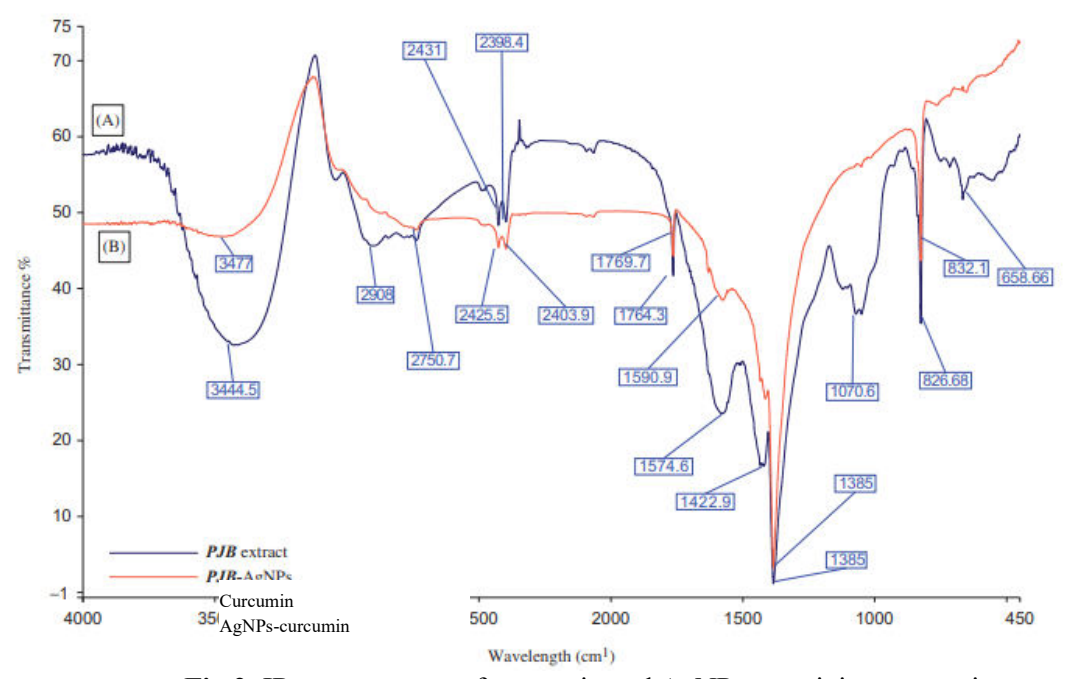


Fig 2: IR spectroscopy of curcumin and AgNPs containing curcumin

4.4 pH and viscosity

The outcomes demonstrated that the method used to manufacture the hydrogel formulations for this investigation could yield formulations with consistent drug concentration and low variability. Table 2 displays each honey-hydrogel's pH value. The pH of the hydrogel formulations was found to be between 5.3 and 7.8, which is within the typical range of the skin. This suggests that the formulations are suitable for application on the skin without causing irritation. The spreadability characteristic determines how evenly a paste is applied to the skin; a high-quality paste will spread quickly. (12)

4.5 Spreadability and swelling index

Spreadability aids in the consistent application of gel to the skin and is crucial for patient compliance. The optimal formulation's spreadability was determined to be 8.6 ± 0.03 , as indicated in Table 2. For every formulation (F1–F8), the swelling index was calculated, first after one hour and then up to three hours (Table 3). Despite this, it was noted that all formulations exhibited quick swelling because the hydrogels' wide surface area and porous structure allowed the solvent to absorb quickly. This could be explained by the polymer's viscosity, which significantly influenced the process of swelling. The relationship between swelling and the kind of polymer, level of cross-linking, ionic strength, and presence of water was also revealed by the results. Due to the creation of a tighter structure, an increase in cross-linker concentration directly affects the hydrogel swelling index negatively. This is consistent with our findings as hydrogels based on the high cross-linker polymer carbopol 934 had the lowest swelling index values, which ranged from 15% to 33%w/w.(13)

Table 3: Evaluation of AgNPs loaded hydrogel

Sl. No	Formulation	Homogeneity	pН	Viscosity	Spreadability
1	HF1		5.8 ± 0.01	0.63 ± 0.10	8.2 ± 0.03
2	HF2		6.3 ± 0.03	2.35 ± 0.15	8.9 ± 0.02
3	HF3		5.7 ± 0.02	6.86 ± 0.09	7.9 ± 0.01
4	HF4	Homogeneous	5.5 ± 0.03	8.43 ± 0.15	8.0 ± 0.04
5	HF5		6.1 ± 0.04	3.15 ± 0.25	7.9 ± 0.02
6	HF6		5.8 ± 0.03	6.45 ± 0.09	7.7 ± 0.03
7	HF7		6.0 ± 0.02	9.26 ± 0.15	7.6 ± 0.01
8	HF8		6.1 ± 0.03	11.16 ± 0.25	7.5 ± 0.01

Table 4: Characterization of optimized hydrogel patches

Optimized Formulation	Equilibrium swelling ratio (%)	Gel content (%)	Thickness (mm)
HF4	46.53±2.89	72.8±3.48	0.357 ± 0.009

4.6 Release kinetics of hydrogel patches

The release profile of curcumin from silver nanoparticle loaded hydrogel were studied at phosphate buffer pH 7.4. Approximately 10 mg of curcumin loaded silver nanoparticle incorporated hydrogel were incubated in 50 ml of buffer pH 7.4 at $37\pm0.5^{\circ}$ C at 75 rpm. After predetermined time interval of 0, 1, 2, 3, 4, 5, 6 hr, 5 ml of sample was withdrawn and replaced by 5 ml of fresh media. Optical density of each sample wasmeasured using UV spectrophotometer at λ max 430 nm for curcumin. A control experiment to determine the release behavior of the free curcumin was also performed. An appropriate amount of curcumin was dissolved in phosphate buffer pH 7.4 and same volume of this solution was placed in dialysis membrane temperature maintained at 37 ± 0.5 °C. Each experiment was performed in triplicate (n=3). The release kinetics of the hydrogelshowed to follow Korsmeyer Peppas model. (21)

Table 5: a) zero order release kinetic, b) First Order release kinetic, c) Higuchi model of release kinetics, d) Korsmeyer peppas model of release kinetics for release of curcumin from AgNPs loaded hydrogel patch

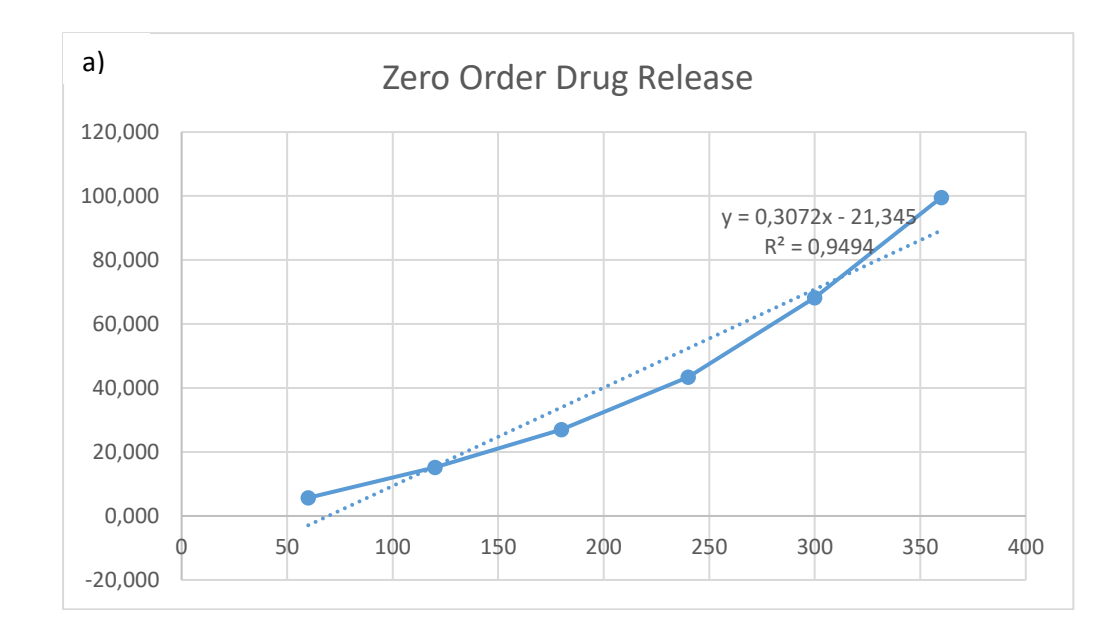
a) %cumulative Time (min) Drug release **60** 5.690 120 15.142 180 26.950 240 43.420 300 68.235 360 99.563

b)	
Time	Log % drug
(min)	release
60	0.755
120	0.976
180	1.072
240	1.217
300	1.395
360	1.496

c) d)

√Time	%cumulative Drug release
7.745967	5.690
10.95445	15.142
13.41641	26.950
15.49193	43.420
17.32051	68.235
18.97367	99.563

Log	Log %
time	cumulative drug
	release
1.78	0.7551
2.08	1.1802
2.26	1.4306
2.38	1.6377
2.48	1.8340
2.56	1.9981



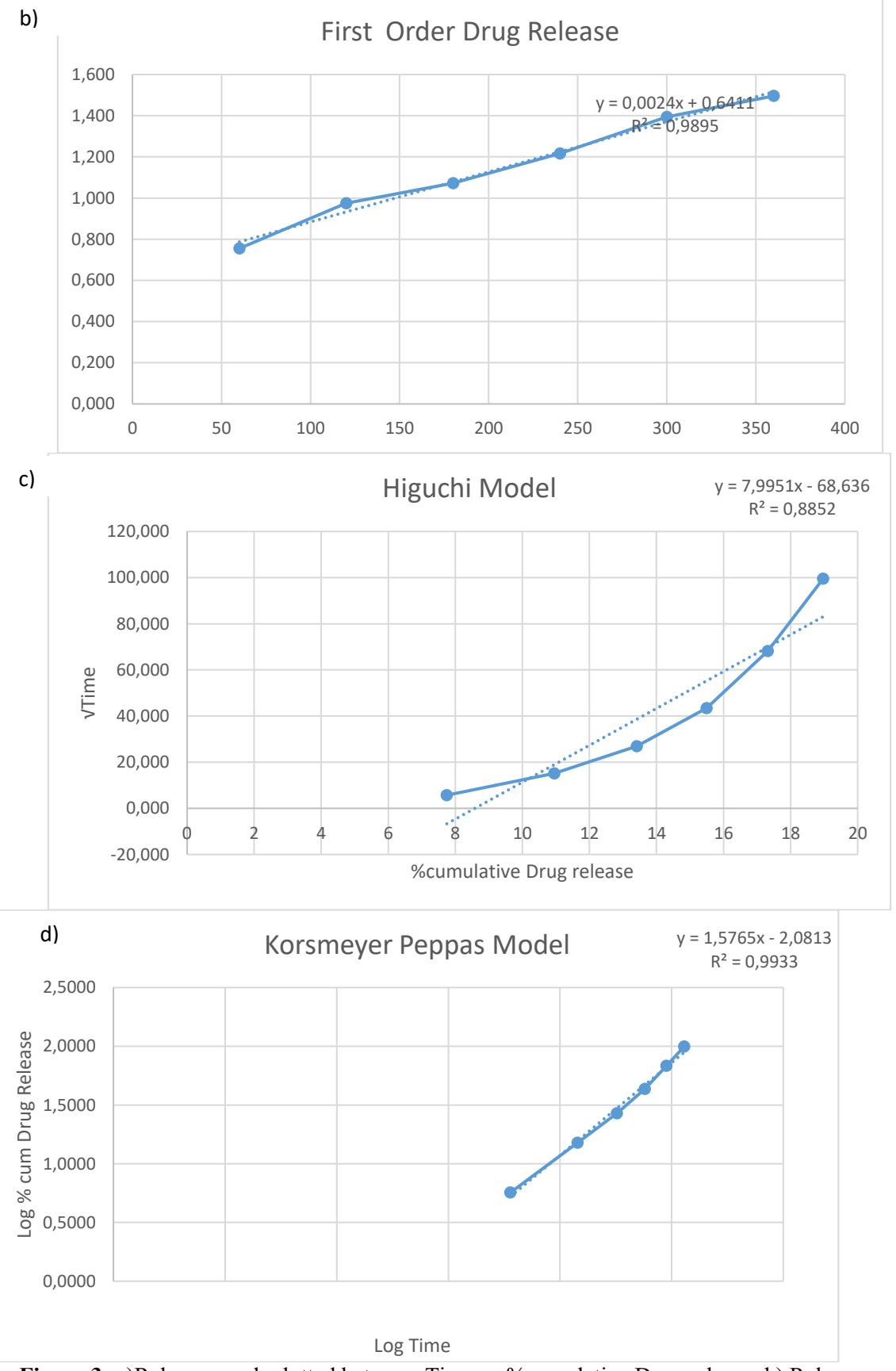


Figure 3: a)Release graph plotted between Time vs %cumulative Drug release. b) Release graph plotted between time vs Log % drug release. c) Release graph plotted between √Time and

%cumulative Drug release. d) Release graph plotted between Log time and Log % cumulative drug release.

4.7 Wound Healing Activity:

Table 6:Effect of Silver nano particles on excision wound model.

Groups	% Wound cor	Epithelisati on period (Days)				
	3 th day	6 th day	9 th day	12 th day	15 th day	(Days)
Control	16.01±2.53	31.59±4.54	46.75±2.75	71.59±4.31	88.12±4.41	16.5±0.84
Standard	29.8±4.42	45.89±1.35 a*	72.48±5.23 a**	92.96±3.14 a**	100a*	13.16±0.54 a*
Silver nano particles (Test-1)	30.12±5.09 a**	41.82±2.56 a**	70.14±5.25 a**	90.31±2.96 a***	98.12±2.42a *	12.83±0.7a*
Silver nano particles (Test-2)	32.59±4.54	45.96±1.43 a*	71.59±4.31 a*	93.02±3.66 a**	100a*	13.33±0.61a *

Values are mean ± SEM from a group of four animals. *p<0.05,**p<0.01 and***p<0.001

- a- Significance difference in compare to untreated group
- **b-** Significance difference in compare to standard treated group

Table 7:Effect of Silver nano particles loaded hydrogel patchon incision wound model.

Groups	Treatment	Wound breaking strength (g)
Ι	Control (Untreated)	165.5±3.43
II	Standard (Intadine treated)	200.73±6.56a***
III	Hydrogel patch with curcumin (Test-1)	181.25±4.53a**
IV	Hydrogel patch loaded with AgNPs containing	195.48±6.78a***
	curcumin (Test-2)	

Values are mean ± SEM from a group of four animals**p<0.01,***p<0.001

- a- Significance difference in compare to untreated group
- **b-** Significance difference in compare to standard treated group

Wound healing involves a cascade of events characterized by completion of biological processes in a certain order and a certain time frame. These events represent the restructuring of the damaged tissue in an attempt to restore as normal a condition as is possible. The natural response of a living organism is to repair the wounds in the shortest time possible and to re-establish the normal continuum of the structure.

Tensile strength of wound represents the promotion of wound healing. Usually, wound healing agents promote the gaining of Tensile strength. Tensile strength (the force required to open the healing skin) was used to measure the amount of healing.

The studies on excision wound healing model reveal that all the groups showed day to day decrease in wound area. However, on 15th post wounding day, control animals' group-I showed 88.12% of wound contraction whereas group-II standard group animals, showed that of 100% and Silver nano particles treated group-III & IV exhibited that of 98.12 & 100% wound contraction respectively. When compared with the standard, the activity of gel was found to be slightly lesser. It was also observed that reducing the epithelization period of Silver nano particles (12.83 & 13.33) treated group in comparison to control group (Table 6). The time required for complete epithelization of the excision wound is an important parameter to assess the wound healing process.

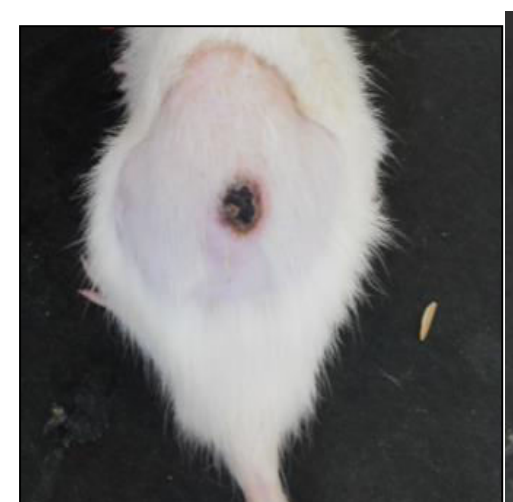
The promotion of wound healing activity is also well gazed by its tensile strength of the incision wound. Generally, wound-healing agents have the properties to enhance the deposition of collagen content, which provides strength to the tissues and forms cross-linkages between collagen fibres. The tensile strength of the Silver nano particles treated groups was found to be (181.25 & 195.48) which was higher than that of control group (165.5) and slightly lesser than that of standard group (200.73) of animals on 15th post wounding day, which indicate good wound healing strength of the Silver nano particles (Table 7).

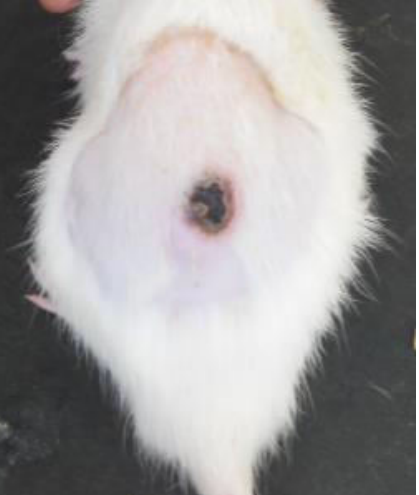
4.8 Excision model

Control Group







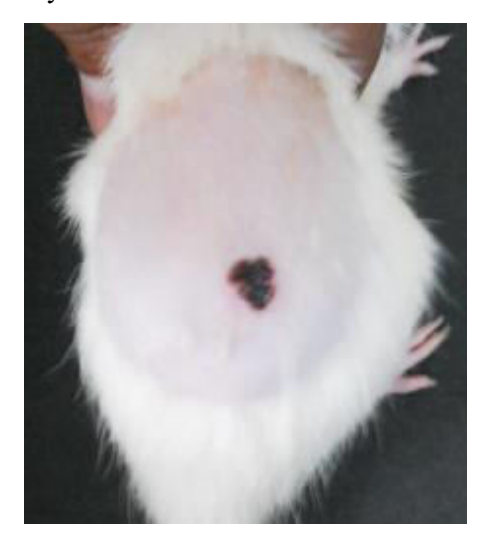


Day 6 Day 9

Day 12



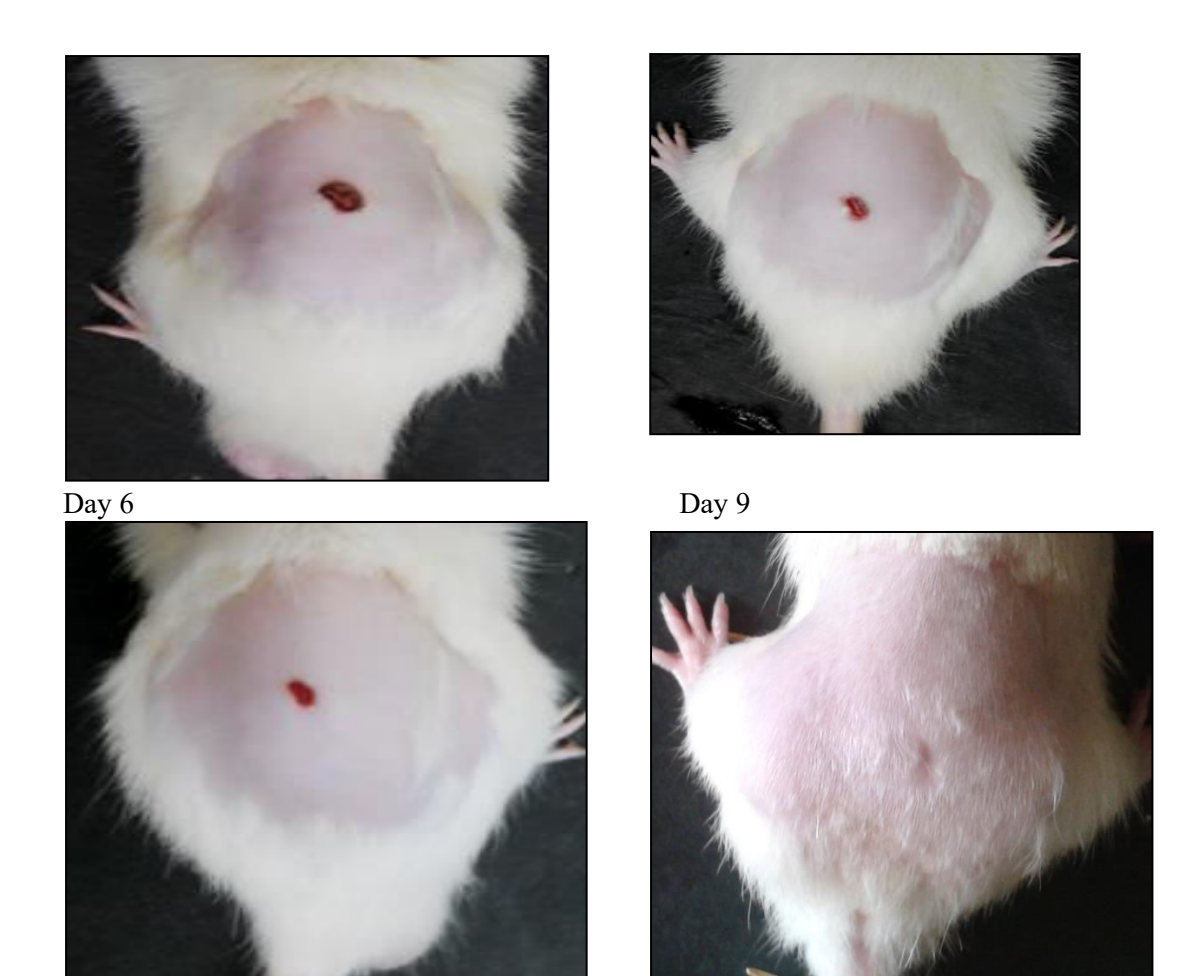
Day 15



Standard



Day 1 Day 3



Test I

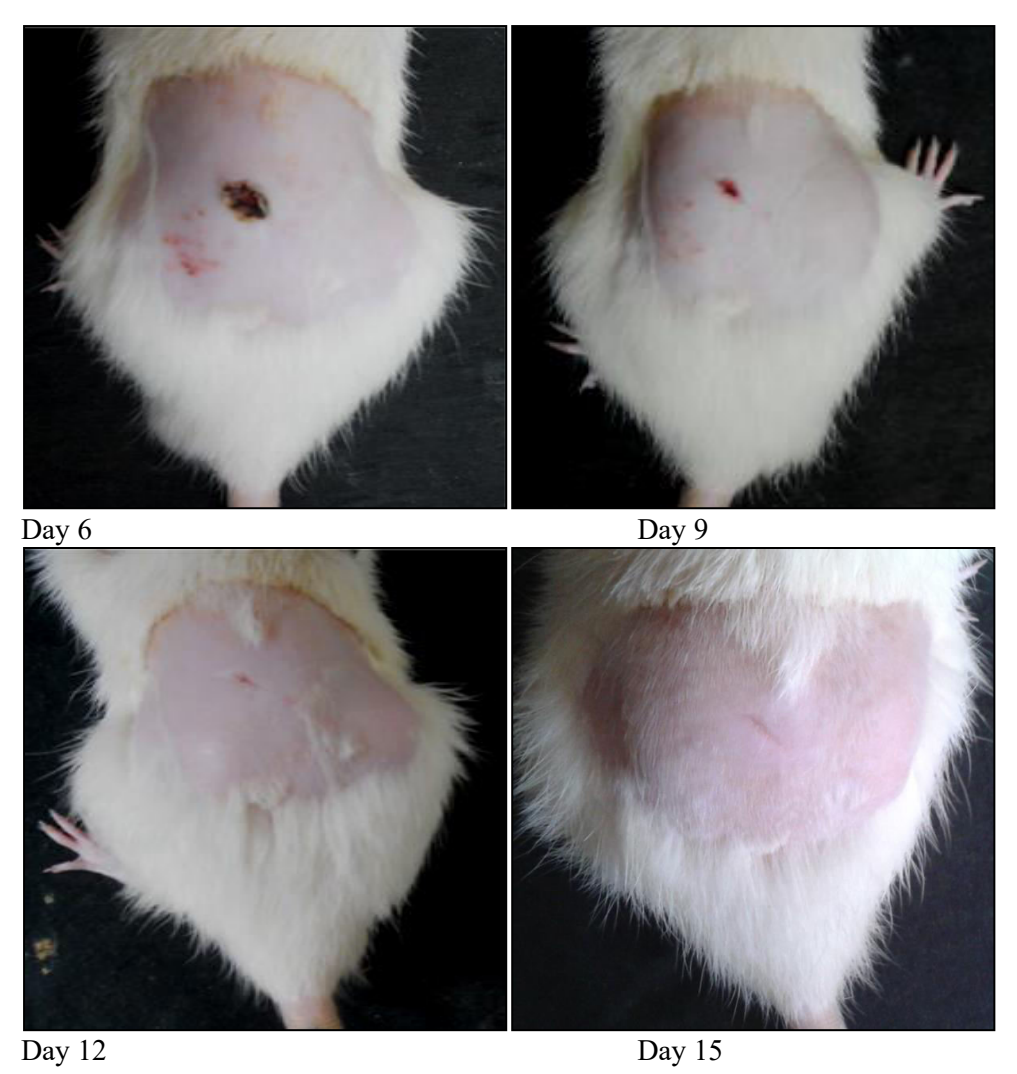
Day 12





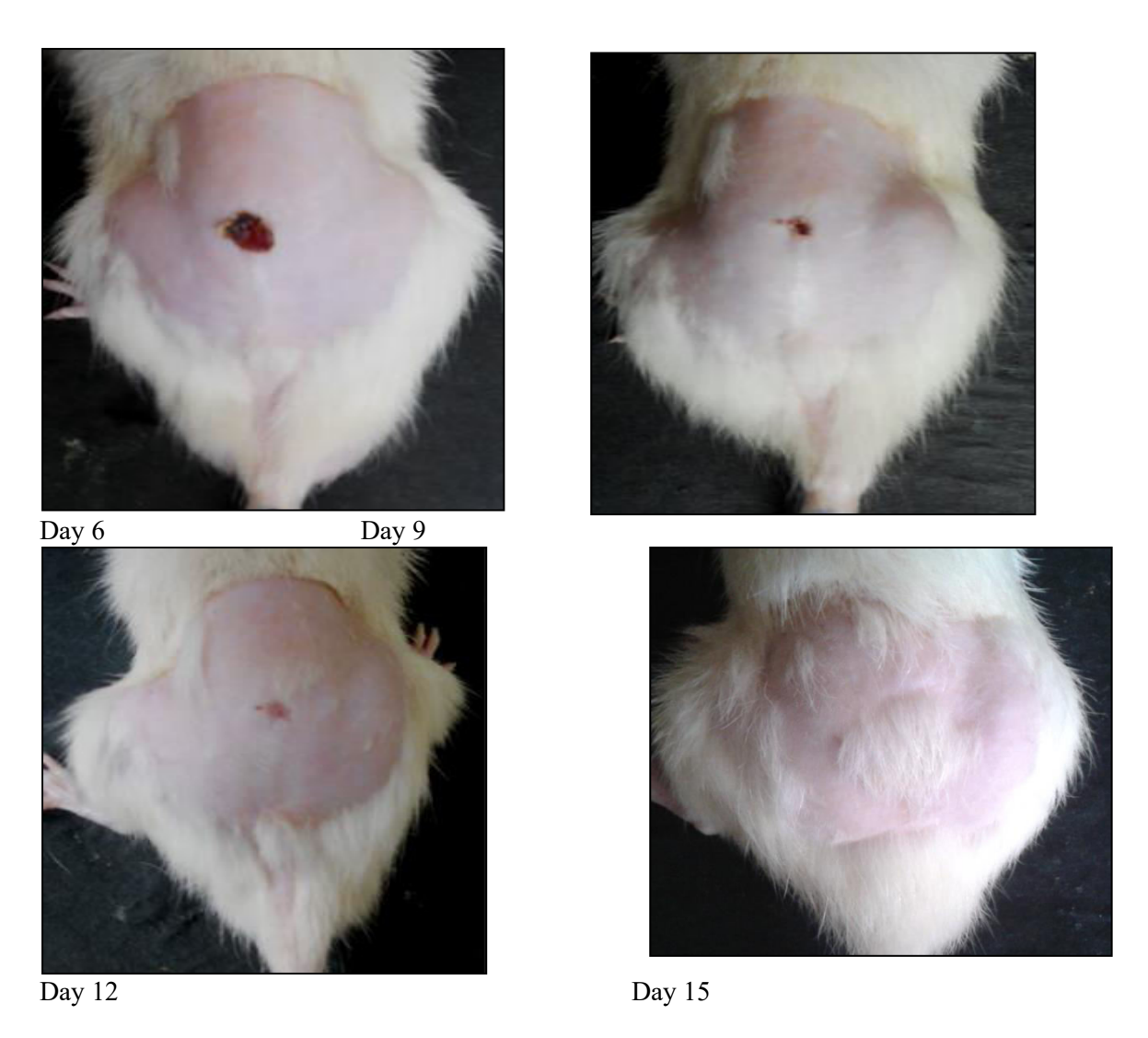
Day 15



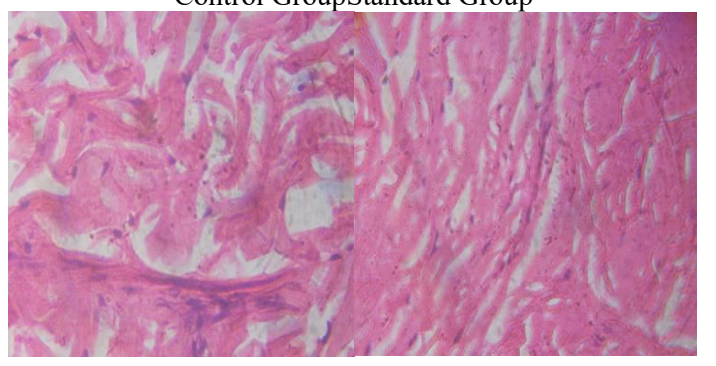








4.9 Incision modelControl GroupStandard Group



Test I Test II

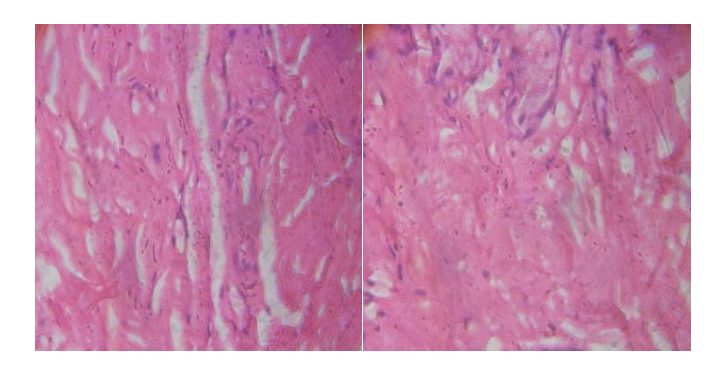


Fig 4: Histopathological examination of different group of treatment

5. Conclusion:

The current study successfully formulated a hydrogel containing silver nanoparticles (AgNPs) loaded with curcumin, aiming to evaluate wound healing activities. Silver nanoparticles were synthesized through a reduction method using silver nitrate, tri-sodium citrate as a stabilizer, and sodium borohydride as a reducing agent. The formation of AgNPs was confirmed by the color change to pale yellow. The nanoparticles, isolated and lyophilized, were characterized with an average size of 54 nm, polydispersity index of 0.2, and a zeta potential of -16 mV. Optimization of the formulation was achieved with specific concentrations of AgNO₃, TSC, and NaBH4, resulting in a particle size of 54.3 nm and entrapment efficiency of 75.2%.

FTIR analysis confirmed the successful loading and interaction of curcumin with AgNPs, indicating phenolic and amine groups involved in the capping and stabilization of nanoparticles. The AgNPs were incorporated into a carbopol hydrogel, which exhibited favorable physicochemical properties, including a pH range between 5.3 and 7.8, and optimal spreadability. The hydrogel followed the Korsmeyer-Peppas release model, showing a sustained release of curcumin at pH 7.4.

In vivo wound healing studies using an excision model demonstrated significant wound contraction, with AgNP-treated groups achieving up to 100% contraction by day 15. Tensile strength measurements further supported the enhanced wound healing, with the AgNP-treated groups showing improved tensile strength compared to the control group. Overall, the formulation showed effective wound healing potential, though slightly lower than the standard treatment. Future studies could focus on enhancing drug release and incorporating other natural ingredients for improved therapeutic efficacy.

6. References:

- 1. Oliveira A, Simões S, Ascenso A, Reis CP. Therapeutic advances in wound healing. Journal of Dermatological Treatment. 2022;33(1):2–22.
- 2. Jiang Y, Fu X, Lu S, Niu Y, Wang Q, Xie T, et al. Tissue Repair and Regeneration Disorders: Repair and Regeneration of Chronic Refractory Wounds. Regenerative Medicine in China. 2021 Jan 1:139–78.
- 3. Basu S, Shukla V. Complications of wound healing. Measurements in Wound Healing: Science and Practice. 2013 Aug 1;109–44.
- 4. Eming SA, Martin P, Tomic-Canic M. Wound repair and regeneration: Mechanisms, signaling, and translation. SciTransl Med. 2014 Dec 3;6(265).
- 5. Nqakala Z, Sibuyi N, FadakaA, ... MMI journal of, 2021 undefined. Advances in nanotechnology towards development of silver nanoparticle-based wound-healing agents. mdpi.com [Internet]. [cited 2024 Oct 20]; Available from: https://www.mdpi.com/1422-0067/22/20/11272
- 6. Paladini F, Materials MP, 2019 undefined. Antimicrobial silver nanoparticles for wound healing application: progress and future trends. mdpi.com [Internet]. [cited 2024 Oct 20]; Available from: https://www.mdpi.com/1996-1944/12/16/2540
- 7. Konop M, Damps T, Misicka A, Rudnicka L. Certain Aspects of Silver and Silver Nanoparticles in Wound Care: A Minireview. J Nanomater. 2016;2016.
- 8. Wilkinson L, White R, care JCJ of wound, 2011 undefined. Silver and nanoparticles of silver in wound dressings: a review of efficacy and safety. magonlinelibrary.com [Internet]. 2011

- [cited 2024 Oct 20];20(11):543–9. Available from: https://www.magonlinelibrary.com/doi/abs/10.12968/jowc.2011.20.11.543
- 9. Dawadi S, Katuwal S, nanomaterials AG... of, 2021 undefined. Current research on silver nanoparticles: synthesis, characterization, and applications. Wiley Online Library [Internet]. [cited 2024 Oct 20]; Available from: https://onlinelibrary.wiley.com/doi/abs/10.1155/2021/6687290
- 10. Ahmed S, Ahmad M, Swami B, research SIJ of radiation, 2016 undefined. Green synthesis of silver nanoparticles using Azadirachtaindica aqueous leaf extract. ElsevierS Ahmed, M Ahmad, BL Swami, S IkramJournal of radiation research and applied sciences, 2016•Elsevier [Internet]. [cited 2024 May 16]; Available from: https://www.sciencedirect.com/science/article/pii/S1687850715000734
- 11. Thakre N, Tiwari G, ... NGF in H, 2024 undefined. Bioactive Hydrogel Patch loaded with curcumin containing Silver Nanoparticles for Enhanced Antimicrobial activity. healthinformaticsjournal.com [Internet]. 2024 [cited 2024 Nov 4];13(3):806–27. Available from: https://healthinformaticsjournal.com/index.php/IJMI/article/view/123
- 12. Alaqad K, ToxicolTSJEnvironAnal, 2016 undefined. Gold and silver nanoparticles: synthesis methods, characterization routes and applications towards drugs. academia.edu [Internet]. 2016 [cited 2024 Oct 20];6:384. Available from: https://www.academia.edu/download/58174105/gold-and-silver-nanoparticles-synthesis-methods-characterizationroutes-and-applications-towards-drugs-2161-0525-1000384.pdf
- 13. Almatroudi A. Silver nanoparticles: Synthesis, characterisation and biomedical applications. Open Life Sci. 2020 Jan 1;15(1):819–39.
- 14. Khan Z, Al-Thabaiti SA, Obaid AY, Al-Youbi AO. Preparation and characterization of silver nanoparticles by chemical reduction method. Colloids Surf B Biointerfaces. 2011 Feb 1;82(2):513–7.
- 15. Lal S, Jana U, Manna PK, Mohanta GP, Manavalan R, Pal SL. Nanoparticle: An overview of preparation and characterization. japsonline.comSL Pal, U Jana, PK Manna, GP Mohanta, R ManavalanJournal of applied pharmaceutical science, 2011•japsonline.com [Internet]. [cited 2024 May 17];2011(06):228–34. Available from: https://japsonline.com/abstract.php?article_id=159&sts=2
- 16. Rivera-Rangel R, ... MGMC and SA, 2018 undefined. Green synthesis of silver nanoparticles in oil-in-water microemulsion and nano-emulsion using geranium leaf aqueous extract as a reducing agent. ElsevierRD Rivera-Rangel, MP González-Muñoz, M Avila-Rodriguez, TA Razo-Lazcano, C SolansColloids and Surfaces A: Physicochemical and Engineering Aspects, 2018•Elsevier [Internet]. [cited 2024 May 16]; Available from: https://www.sciencedirect.com/science/article/pii/S0927775717307008
- 17. Gurunathan S, Kalishwaralal K, Vaidyanathan R, Venkataraman D, Pandian SRK, Muniyandi J, et al. Biosynthesis, purification and characterization of silver nanoparticles using Escherichia coli. Colloids Surf B Biointerfaces. 2009 Nov 1;74(1):328–35.
- 18. Shafaghat A. Synthesis and characterization of silver nanoparticles by phytosynthesis method and their biological activity. Synthesis and Reactivity in Inorganic, Metal-Organic and Nano-Metal Chemistry. 2015;45(3):381–7.
- 19. Mukherji S, Bharti S, Shukla G, Mukherji S. Synthesis and characterization of size- And shape-controlled silver nanoparticles. Physical Sciences Reviews. 2019 Jan 1;4(1).
- 20. Dawadi S, Katuwal S, Gupta A, Lamichhane U, Thapa R, Jaisi S, et al. Current Research on Silver Nanoparticles: Synthesis, Characterization, and Applications. J Nanomater. 2021;2021.
- 21. Quintero-Quiroz C, Acevedo N, Zapata-Giraldo J, Botero LE, Quintero J, Zárate-Trivino D, et al. Optimization of silver nanoparticle synthesis by chemical reduction and evaluation of its antimicrobial and toxic activity. Biomater Res. 2019 Dec 19;23(1).
- Vigata M, Meinert C, Hutmacher D, Pharmaceutics NB, 2020 undefined. Hydrogels as drug delivery systems: A review of current characterization and evaluation techniques. mdpi.com [Internet]. [cited 2024 Oct 20]; Available from: https://www.mdpi.com/1999-4923/12/1188

- 23. Van Den Bulcke AI, Bogdanov B, De Rooze N, Schacht EH, Cornelissen M, Berghmans H. Structural and rheological properties of methacrylamide modified gelatin hydrogels. Biomacromolecules. 2000;1(1):31–8.
- 24. El-Kased R, Amer R, Attia D, reports MES, 2017 undefined. Honey-based hydrogel: In vitro and comparative In vivo evaluation for burn wound healing. nature.com [Internet]. [cited 2024 Oct 20]; Available from: https://www.nature.com/articles/s41598-017-08771-8
- 25. Bellingeri R, Alustiza F, Picco N, Acevedo D, Molina MA, Rivero R, et al. In vitro toxicity evaluation of hydrogel–carbon nanotubes composites on intestinal cells. Wiley Online Library [Internet]. 2014 Feb 1 [cited 2024 Oct 20];132(5):41370. Available from: https://onlinelibrary.wiley.com/doi/abs/10.1002/app.41370
- 26. Garg S, Res AGIJPS, 2018 undefined. Encapsulation of curcumin in silver nanoparticle for enhancement of anticancer drug delivery. researchgate.netS Garg, A GargInt J Pharm Sci Res, 2018•researchgate.net [Internet]. [cited 2024 Jul 24]; Available from: https://www.researchgate.net/profile/Ashish-Garg-20/publication/324570080_encapsulation_of_curcumin_in_silver_nanoparticle_for_enhancement_of_anticancer_drug_delivery/links/5ad6071c0f7e9b2859376ed4/encapsulation-of-curcumin-in-silver-nanoparticle-for-enhancement-of-anticancer-drug-delivery.pdf
- 27. Qadri S, animals SRL, 2018 undefined. Laws, regulations, and guidelines governing research animal care and use in India. Elsevier [Internet]. [cited 2024 Oct 20]; Available from: https://www.sciencedirect.com/science/article/pii/B9780128498804000088
- 28. Quazi A, Patwekar M, Patwekar F, Mezni A, Ahmad I, Islam F. Evaluation of Wound Healing Activity (Excision Wound Model) of Ointment Prepared from Infusion Extract of Polyherbal Tea Bag Formulation in Diabetes-Induced Rats. Evidence-based Complementary and Alternative Medicine. 2022;2022.
- 29. Singh VP, Yadav S. Ethics, Animal Welfare and Regulation: The Indian Perspective. Essentials of Laboratory Animal Science: Principles and Practices. 2021 Jan 1;39–51.
- 30. Lin SP, Lo KY, Tseng TN, Liu JM, Shih TY, Cheng KC. Evaluation of PVA/dextran/chitosan hydrogel for wound dressing. Cellular Polymers. 2019 Jan 1;38(1–2):15–30.
- 31. El-Kased RF, Amer RI, Attia D, Elmazar& MM. Honey-based hydrogel: In vitro and comparative In vivo evaluation for burn wound healing. [cited 2024 Aug 20]; Available from: www.nature.com/scientificreports/